International Journal of Non-Linear Mechanics 91 (2017) 189–197

Contents lists available at ScienceDirect

International Journal of Non-Linear Mechanics

journal homepage: www.elsevier.com/locate/nlm

Functionally graded rod with small concentration of inclusions: Homogenization and optimization

Igor V. Andrianov[a], Jan Awrejcewicz[b,c,*], Alexander A. Diskovsky[d]

[a] Institut für Allgemeine Mechanik, RWTH Aachen University, Templergraben 64, D-52056 Aachen, Germany
[b] Department of Automation, Biomechanics and Mechatronics, Lodz University of Technology, 1/15 Stefanowskiego St., PL-90924 Lodz, Poland
[c] Department of Vehicles, Warsaw University of Technology, 84 Narbutta Str., PL-02524 Warsaw, Poland
[d] National Metallurgical Academy of Ukraine, Department of Higher Mathematics, Gagarina 23, UA-49005 Dnepr, Ukraine

ARTICLE INFO

Keywords:
Rod
Beam
Functionally graded structure
Functionally graded material
Inclusion
Homogenization
Optimization

ABSTRACT

This work is devoted to strain analysis and optimal design of a Functionally Graded (FG) rods and beams with small inclusions. The homogenization procedure plays a key role in our investigations. The method is illustrated using an example of the rod longitudinal deformation and bending of a beam. We consider the cases of FG inclusion sizes and FG steps between inclusions separately. Particular problems of optimal design are discussed in some details. The mathematical model of the bending beam, which adapts to the external load action, is proposed and an illustrative example of the adaptation process is given.

1. Introduction

The mechanical response of materials with spatial gradients in composition and structure is of considerable interest in numerous and diverse disciplines, such as tribology [1], geology [2,3] optoelectronics, biomechanics [4,5], fracture mechanics [6], and nanotechnology [7,8]. A fundamental approach allowing for deduction of the macro-scale laws and the constitutive relation by proper homogenization over the micro-scale is known as the homogenization method [9–17]. This method is also successfully used for modeling and simulating mechanical behavior of the FG Materials (FGM) [18,19] and the Functionally Graded Structures (FGS). Typically the term FGS is associated with the constructions made/fabricated from FGM. However, in this paper, the term FGS is understood in a broader manner, since the heterogeneous constructions with a controlled heterogeneity parameter are also taken into account (for instance, the reinforced plates and shells with nonuniformly distributed ribs of different stiffness; goffer-type constructions consisting of different amplitudes of goffer shapes and their half-wave length, etc. [20–25]). FGMs are composites consisting of two different materials with a gradient composition. In the case of application of the homogenization method, the coefficients of periodic composites state equations are usually [9–13] approximated by the first terms of their Fourier series (Fig. 1a). In a similar way [20–25], the coefficients of FGSs state equations with FG inclusion sizes (Fig. 1b) and FG step between the inclusions (Fig. 1c) can be approximated.

However, the truncated Fourier series (even for a small number of terms) relatively well approximate the coefficients of the constitutive equations for large concentration of inclusions (fibres, ribs, etc.), when the distance between inclusions is of the same order as their typical sizes. However, for small concentration, when the distance between inclusions is essentially larger than their size, the constitutive equation coefficients are approximated by impulse periodic function (see, for instance, Fig. 1d). In this case, a usual homogenization procedure may be accompanied by some problems to be directly applied.

Therefore, for a small concentration of inclusions, it is recommended to use the further presented variant of homogenization method, where small sizes of the inclusions with respect to the distance between them are utilized to employ the asymptotic procedure. Modifications of this approach for FGS with small inclusion concentrations are also proposed.

The applied method is illustrated using a relatively simple problem, i.e., we consider a rod with a longitudinal strain. In our investigations, the rod diameter is taken commensurable with inclusions sizes.

2. FG inclusion sizes

FG properties can be achieved, for instance, by applying different inclusion sizes. Let us analyze an influence of different sizes of inclusions on the longitudinal rod stiffness, keeping the distance between inclusions (Fig. 2) constant. We define changes of the inclusion

* Corresponding author.
E-mail addresses: igor_andrianov@hotmail.com (I.V. Andrianov), awrejcew@p.lodz.pl (J. Awrejcewicz), alex_diskovskiy@ukr.net (A.A. Diskovsky).

http://dx.doi.org/10.1016/j.ijnonlinmec.2017.02.007
Received 26 February 2016; Received in revised form 9 February 2017; Accepted 11 February 2017
Available online 13 February 2017

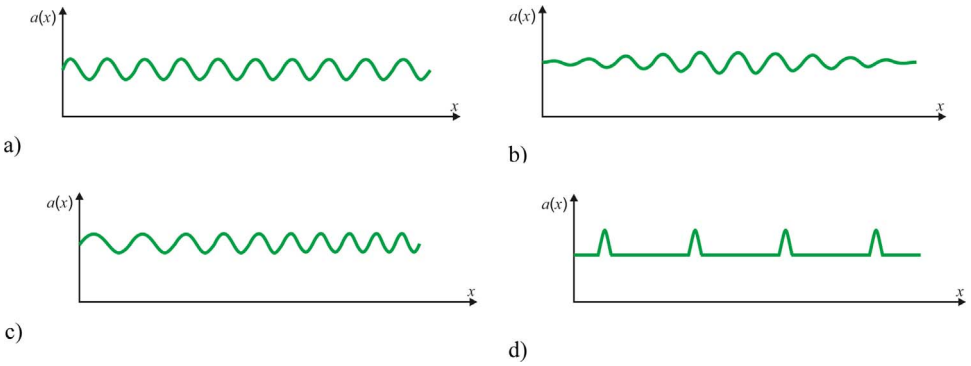

Fig. 1. Schematic view of the constitutive equation coefficient $a(x)$for a composite: a) periodic structure; b) FG inclusion sizes; c) FG steps between inclusions; d) small inclusion concentration.

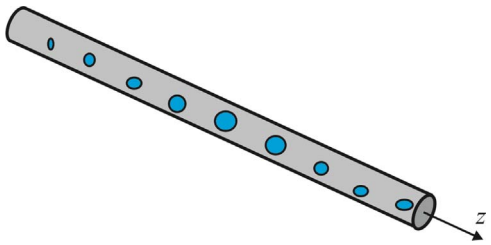

Fig. 2. Schematic view of the rod with FG sizes of inclusions.

dimensions by a function $V = V(x)$.

In what follows, we consider a deformation of the FGM rod subjected to the spatially distributed load $P(z)$ and the inclusions (Fig. 2) by being equivalent to concentrated elastic elements (Fig. 3). Observe that for composites with regular structure, the analogous models of two-component rod are applied (see references [26–28]).

Obviously, a number of n is large, and hence the distance $l = z_i - z_{i-1}$ between them is much less than the rod length L, $l \ll L$. Therefore, in order to investigate the longitudinal deformation of the two-component rod (Fig. 3), one may apply the following variant of the homogenization procedure.

Equilibrium equation of the rod part between the concentrated elastic elements has the following form

$$\frac{d^2u}{dx^2} = p, \tag{1}$$

where: $x = z/l$; $u = v/l$; v is the longitudinal displacement; $p = \frac{P(lx)}{lk_0}$; $k_0 = E_0F$; E_0 is Young's modulus of the rod material; F is the cross section area.

Since the approximate inclusions composed of the elastic elements can be treated as discrete elastic cross sections, the associated compatibility conditions regarding the i-th inclusion follow

$$(u)^+ = (u)^-; \quad \left(\frac{du}{dx}\right)^+ - \left(\frac{du}{dx}\right)^- = ku, \tag{2}$$

where $(\ldots)^- = \lim_{x=i-0}(\ldots); (\ldots)^+ = \lim_{x=i+0}(\ldots)$; $k = \frac{lk_1(x)}{k_0}$; k_1 is the stiffness of the discrete elastic inclusions.

3. Homogenization procedure for longitudinal deformation

Owing to the homogenization approach, let us introduce the "fast" variable ξ

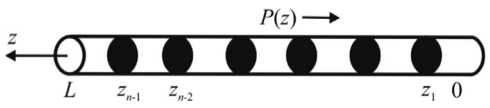

Fig. 3. Schematic view of the two-component rod with concentrated elastic elements.

$$\xi = x/\varepsilon, \tag{3}$$

where $\varepsilon = 1/n \ll 1$.

We treat the variables x and ξ as independent ones, and the differential operator used in (1), (2) has the following form

$$\frac{d}{dx} = \frac{\partial}{\partial x} + \varepsilon^{-1}\frac{\partial}{\partial \xi}. \tag{4}$$

Displacement u can be presented in the following form

$$u = u_0(x) + \varepsilon^2 u_1(x, \xi) + \varepsilon^3 u_2(x, \xi) + \ldots, \tag{5}$$

where u_s $(s = 1,2,\ldots)$ is a periodic function with respect to ξ with period n.

Substituting Ansatzes (4), (5) into Eq. (1) and compatibility condition (2) and carrying out the splitting with respect to ε, the following homogenized equation describing the longitudinal displacement of the two-component rod is obtained

$$\frac{d^2u_0}{dx^2} + k(x)u_0 = p. \tag{6}$$

Micromechanical effects are described by the functions u_s $(s = 1,2, \ldots)$. For the function u_1 on the period $\xi \in (0, n)$one obtains:

$$\frac{\partial u_1}{\partial \xi} = k(x)u_0\left(\xi - \frac{n}{2}\right). \tag{7}$$

Next, the function u_1 is periodically extended along the whole rod length.

4. Inverse problem

The main advantage of the proposed approach is that it allows to efficiently solve the problems of optimization, i.e., problems devoted to determination of optimal characteristics of the internal material structure protecting the given structure properties. In the studied case of the FG amplitudes, the target characteristic is the function $V = V(x)$ governing a rule of the inclusion sizes change. As an example we consider the problem of determination of the function $V(x)$ that provides the largest longitudinal stiffness of the rod under a given load.

It is convenient to rather take the function $k(x)$ as the control function instead of the function $V(x)$.

Without loss of generality, let us take the boundary conditions in the following form

$$u|_{x=0} = 0, \quad \frac{du}{dx}|_{x=n} = 0. \tag{8}$$

In order to measure the rod stiffness properties, we take energy of the elastic deformations and use zero-order approximation of the displacement (5). Then, we define a minimum of the following functional

$$I = \int_0^n p u_0 dx \to \min_k. \tag{9}$$

One can introduce the following isoperimetric condition which guarantees constant total stiffness inclusions

$$\sum_{i=1}^{n-1} k(x_i) = C_d. \tag{10}$$

For large number of inclusions and smooth function $k(x)$, condition (10) can be transformed to the isoperimetric form owing to the application of an Euler-Maclaurin formula [29].

$$\int_0^n k(x)dx = C \approx C_d. \tag{11}$$

In practice, the inclusion sizes meet the technological constrains. Hence, the next constraint for the target function of the following form is required

$$k_{\min} \le k(x) \le k_{\max}. \tag{12}$$

Constraint (12) is satisfied through introduction of the following new control function $\theta(x)$ [30].

$$k = \alpha + \gamma \sin\theta, \tag{13}$$

where: $\alpha = 0.5(k_{\max} + k_{\min})$, $\gamma = 0.5(k_{\max} - k_{\min})$.

Obtaining the function $\theta(x)$ requires solution to the inverse problem (6)–(13):

$$I = \int_0^n p u_0 dx \to \min_\theta, \tag{14}$$

$$I_1 = \gamma \int_0^n \sin\theta dx = \bar{c}, \tag{15}$$

$$\frac{d^2u_0}{dx^2} + (\alpha + \gamma sin\theta)u_0 = p, \tag{16}$$

$$u_0(0) = 0, \qquad \left(\frac{du_0}{dx}\right)_{x=n} = 0, \tag{17}$$

where $\bar{c}$ denotes a constant.

Applying variation of the Lagrange functional of the problem (14)–(17) and introducing the conjugate variable, we get the optimality condition

$$\cos\theta(u_0^2 - \lambda) = 0. \tag{18}$$

As it has been pointed out in Refs. [20–25], the occurrence of singular points belongs to typical problems for optimization of FGS. If one is looking for the control function $\theta(x)$ as a continuous one, then it is impossible to satisfy the first boundary condition in Eq. (17). Therefore, we assume the control function $\theta(x)$ in the form of a piecewise continuous function, which satisfies the following condition on the interval $(0, x_1)$

$$\cos\theta = 0, \tag{19}$$

while on interval (x_1, n) we have

$$u_0^2 - \lambda = 0, \tag{20}$$

where λ stands for the Lagrange multiplier; $x_1(\bar{c})$ denotes the boundary of an area without inclusions.

One gets a coordinate of the point x_1 from the continuity condition of both the function u_0 and its derivative u_{0x} (these conditions are yielded by the Weierstrass-Erdmann conditions [31]):

$$(u_0)^- = (u_0)^+, \qquad \left(\frac{du_0}{dx}\right)^- = \left(\frac{du_0}{dx}\right)^+. \tag{21}$$

The conditions (21), taking into account relations (20), can be written in the following form

$$u_{01}(x_1) = \pm\sqrt{\lambda}, \tag{22}$$

$$\left(\frac{du_{01}}{dx}\right)_{x=x_1} = 0, \tag{23}$$

where u_{01} denotes displacement in the interval $(0, x_1)$. Relations (13), (16), (19) allow to derive the following equation:

$$\frac{d^2u_{01}}{dx^2} + k_{\min}u_{01} = p, \tag{24}$$

with conditions (8), (23). For known u_{01}, conditions (22) allow to obtain x_1. Introducing Ansatz (22) into Eq. (16), we find a formula for $\sin\theta$ in the interval (x_1, n). Then, taking into account relation (13), the following optimal control function is defined

$$k = \begin{cases} k_{\min}, & x \in (0, x_1), \\ \pm\frac{p}{\sqrt{\lambda}}, & x \in (x_1, n). \end{cases} \tag{25}$$

The constant λ is found from an isoperimetric condition (11), which takes the following form

$$\int_{x_1}^n p dx = \pm\sqrt{\lambda}(C - k_{\min}x_1). \tag{26}$$

5. Example of amplitude optimization

In order to illustrate the proposed method, we consider the problems (6)–(12) for linearly distributed load, i.e.,

$$p = \rho x, \tag{27}$$

where:ρ is the positive constant.

Assume that the minimal size of inclusions is equal to zero, i.e.,

$$k_{\min} = 0. \tag{28}$$

Using Eqs. (27), (28) and taking into account the Eq. (24) and boundary conditions (8), (23), one obtains

$$u_{01} = \rho\left(\frac{x^3}{6} - \frac{x_1^2}{2}x\right). \tag{29}$$

Eqs. (22), (27)–(29) give

$$\sqrt{\lambda} = \frac{\rho}{3}x_1^3. \tag{30}$$

Eq. (26), taking into account relations (27), (28), (30), implies the following equation to find x_1:

$$2Cx_1^3 + 3x_1^2 - 3n^2 = 0. \tag{31}$$

Observe that Eq. (31) does not concern an intensity of the load ρ, i.e., x_1 depends only on the applied load character, which is typical for the linear statement formulation. We take the following parameters in order to carry out the numerical simulations: $n = 100$, $C = 10^2, \ldots, 10^3$.

It should be emphasized that for the chosen parameters, Eq. (31) uniquely defines x_1, since among any three roots of the equation, only one is real positive.

The function x_1 versus C is reported in Fig. 4.

Finally, (25) yields the optimal control function

$$k = \begin{cases} 0, & x \in (0, x_1), \\ \frac{3\rho x}{x_1^3}, & x \in (x_1, n). \end{cases} \tag{32}$$

Let us estimate the efficiency of the proposed optimization. For this purpose, we compare the extension of the rod for the optimal stiffness distribution for the equivalent cross section (32) and extension of the rod of the regular form. Extension Δ_0 of the optimal rod can be found from Eqs. (20), (30):

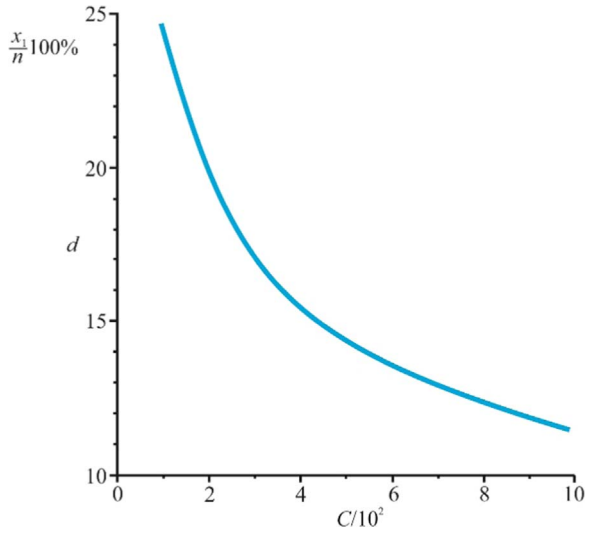

Fig. 4. The function x_1 versus C, $n = 100$.

$$\Delta_0 = \frac{\rho x_1^3}{3}. \tag{33}$$

Integration of Eq. (6) for $k = C/n$, taking into account the boundary conditions (8) and the load (27), yields the following explicit estimating formula for extensions of the regular form rod:

$$\Delta = \frac{\rho n^3}{C}\left(1 - \frac{\tan\sqrt{C}}{\sqrt{C}}\right). \tag{34}$$

With the help of relations (33), (34) we find the relative decrease in the rod extension due to optimal distribution of the inclusions volume

$$\delta = \frac{\Delta - \Delta_0}{\Delta}100\%. \tag{35}$$

For the considered parameters, the relative decrease in the extension δ is of 50%, i.e., for $C = 10^2$, $\delta = 46.6\%$; $C = 5{\cdot}10^2$, $\delta = 49.1\%$; $C = 10^3$, $\delta = 49.7\%$. It should be noted that a small variation δ corresponds to a large difference in summed value of inclusions C. The latter behavior can be explained in the following way. We quantify the relative increase in the stiffness generated only by rearrangement of the inclusion due to the assumed rule. The inclusions stiffness increase is compared with the stiffness of a regular rod having the same inclusions and the same their total magnitude as the investigated functionally graded rod. Obviously, in general, when we consider a linear problem, then variation of δ should not depend on C. The obtained variations of δ are implied by nonlinear equations (for instance (31)) governing a process of the optimized decomposition of inclusions.

6. FG steps between inclusions

Now we will analyze an influence of FG steps between equal inclusions. Consider the basic two-component rod (Fig. 3) with equal elastic inclusions, $k = const$. Assuming a fixed number of inclusions n and $L = n$, we have $l = 1$. Now we change the distance l. In order to describe the rule of the step changes, and following reference [25], we apply a function $f(x)$. This is smooth function with prescribed values in n points:

$$f(x_i) = i, \tag{36}$$

where x_i is a coordinate of the i-th inclusion.

In the problems of optimization of inclusion arrangement, the coordinates of inclusions x_i are unknown to be defined via solution of the employed optimization procedure. It is assumed that our optimization scheme allows us to obtain a continuous function $f(x)$ with the help

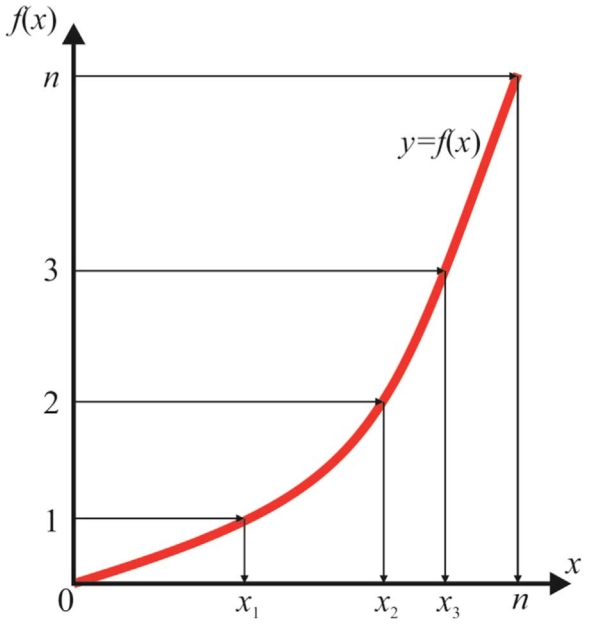

Fig. 5. Nomogram to define coordinates of the i-th elastic inclusion for a given function $f(x)$.

of variational computation. The function $f(x)$ should satisfy the given conditions and assumptions of the used optimization procedure. When the function $f(x)$ is found, the optimal coordinates x_i of inclusions are defined by Eq. (36) for $i = 1, \ldots, n$.

For a constant number of inclusions, the relation between function and coordinates of the inclusions can be found with the help of Fig. 5, which can be treated as a nomogram.

Fig. 5 implies that in order to keep a constant number of inclusions, the function $f(x)$ should have the following properties

$$f(0) = 0, \quad f(n) = n, \quad f'(x) \geq 0. \tag{37}$$

Relation $\Delta f \approx f'(x)\Delta x$ yields the approximation to the steps between inclusions. For the given step $\Delta f = 1$ (Fig. 3), the step of the FG rod $\Delta x = s$ takes the following form

$$s \approx \frac{1}{f'(x)}. \tag{38}$$

7. Direct problem for FG steps

Proceeding in a similar way to that used for the FG inclusion sizes, we consider now the inclusions thickness approaching to zero, and the equations governing the rod deformation with the FG steps take the following form

$$\frac{d^2u}{dx^2} + k\sum_{i=1}^{n-1}\delta(f(x) - i)u = p, \tag{39}$$

where $\delta(x)$ denotes the Dirac delta function.

We introduce the following variable $\eta = f(x)$ $(x = f^{-1}(\eta))$. Therefore, Eq. (39) can be transformed to the following form

$$\frac{d}{d\eta}\left(\frac{du}{\varphi d\eta}\right) + k\sum_{i=1}^{n-1}\delta(\eta - i)\varphi\, u = \tilde{p}, \tag{40}$$

where: $\varphi = \frac{df^{-1}}{d\eta}$, $\tilde{p} = \varphi\, p$.

Eq. (40) is an equation with periodically discontinuous coefficients, and we can apply a homogenization procedure [9]. The equation of equilibrium between inclusions (1) and compatibility conditions (2) for the considered FG steps take the following form

$$\frac{d}{d\eta}\left(\frac{du}{\varphi d\eta}\right) = \tilde{p}, \tag{41}$$

$$(u)_{\eta=i+0} = (u)_{\eta=i-0}, \qquad \left(\frac{du}{\varphi d\eta}\right)_{\eta=i+0} - \left(\frac{du}{\varphi d\eta}\right)_{\eta=i-0} = ku. \tag{42}$$

After introduction of the fast variable $\xi = \eta/\varepsilon$ and applying series

$$u = u_0(\eta) + \varepsilon^2 u_1(\eta, \xi) + \varepsilon^3 u_2(\eta, \xi) + \dots, \tag{43}$$

relations (41), (42) yield the following homogenized equations for u_0:

$$\frac{d}{d\eta}\left(\frac{du_0}{\varphi d\eta}\right) + ku_0 = \tilde{p} \tag{44}$$

and the equation for the correction term u_1:

$$\frac{\partial u_1}{\partial \xi} = k\varphi\, u_0\left(\xi - \frac{n}{2}\right). \tag{45}$$

In the original variable we get

$$\frac{d^2u_0}{dx^2} + kf'(x)u_0 = p. \tag{46}$$

It should be emphasized that the obtained homogenized Eq. (46) represents all physical aspects of the problem. The second term occurring on the left hand side of this equation presents an "additional stiffness" governed by inclusions and continuously distributed along the rod length. In the case of FGS, this distribution is not uniform. In the case of FG steps, denser localization of inclusions involves larger contribution of the "additional stiffness". Mathematically, this property is described by the derivative of the step function $f'(x)$ in Eq. (46).

8. Inverse problem for FG steps

Consider the inverse problem for Eq. (46) with the boundary conditions (8), which uses the following control function

$$\psi = kf'(x). \tag{47}$$

Minimizing functional I represents the energy of the elastic deformation

$$I = \int_0^n u_0 q dx \to \min_\psi. \tag{48}$$

The condition for keeping the number of inclusions (37) constant yields the isoperimetric form for the control function

$$\int_0^n \psi dx = kn. \tag{49}$$

We apply also the technological bounds for ψ, analogous to (12), which will be satisfied automatically after introduction of the control function (13). One may easily verify that the considered inverse problem for the FG rod (46)–(49) coincides with the analogous problem (6)–(12). In what follows, we illustrate how to find the solution to the considered problem.

9. Example of steps optimization

We consider optimization of the steps for the rod (46). Owing to the physical and technological motivations, it is clear that a step/distance between the successive inclusions is subjected to constrains. This is why the function ψ, governing variation of the step between inclusions (38), should obey some constrains in a way similar to the condition (12). In the given example we assume that the following constrain holds

$$\psi_{\min} = 0. \tag{50}$$

It means that inclusions do not appear in the interval $(0, x_1)$, since formula (38) estimating the step between inclusions implies that when condition (50) is satisfied, then the step between inclusions tends to infinity ($s = \infty$). The illustrated requirement (50) yields the particular case considered in Section 5 (for $k = \psi$). Using the control function due to formula (32), the function $f(x)$ is calculated with the help of the condition $f(n) = n$. Eventually we get for load (27)

$$f(x) = \begin{cases} 0, & x \in (0, x_1), \\ \frac{3\rho(x^2 - n^2)}{2x_1^3 k} + n, & x \in (x_1, n). \end{cases} \tag{51}$$

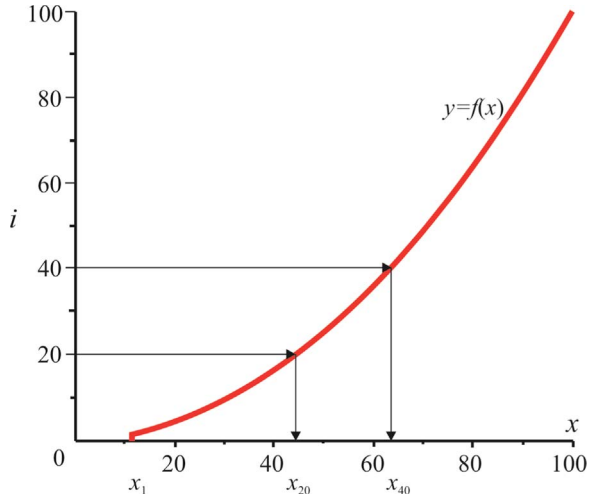

Fig. 6. Nomogram for determination of the optimal coordinates of inclusions providing the largest longitudinal stiffness of the rod under load $q = \rho x$, $\rho \equiv const$.

The function $f(x)$ for $\rho = 100$, $k = 10$, $n = 100$ is shown in Fig. 6.

Introduction of expression (36) into Eq. (51) yields optimal coordinates of the inclusions:

$$x_i = \sqrt{n^2 - \frac{2x_1^3 k(n-i)}{3\rho}}, \tag{52}$$

where: $i = 2, 3, 4, \dots, 100$, and x_1 is defined by Eq. (31).

In Fig. 7 the window enlargement of a part of the nomogram (Fig. 6) is shown for two first inclusions.

The first inclusion coordinate ($x_1 = 11.45$) is found from Eq. (31), whereas the second inclusions coordinate $x_2 = 13.88$ is given by formula (52).

10. Bending of a beam with FG inclusion sizes

We consider bending of a beam with FG inclusion sizes (Fig. 8) loaded by a normal load Q(z). The beam is made of a homogeneous material and has inclusions of varying sizes. The equilibrium equations between successive inclusions follow

$$\frac{d^2M}{dx^2} = q(x), \qquad \frac{d^2w}{dx^2} = \frac{Ml}{E_0 I}, \tag{53}$$

where: M is the bending moment; $x = z/l$; $w = W/l$; W is the beam

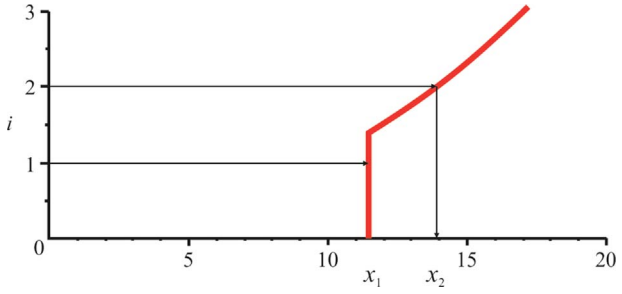

Fig. 7. Nomogram for determination of the coordinates of two first inclusions.

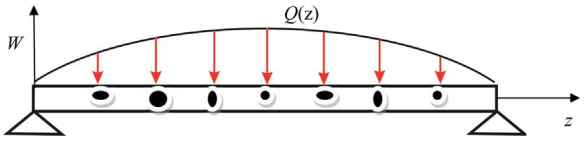

Fig. 8. Schematic view of the bending of the FGM beam.

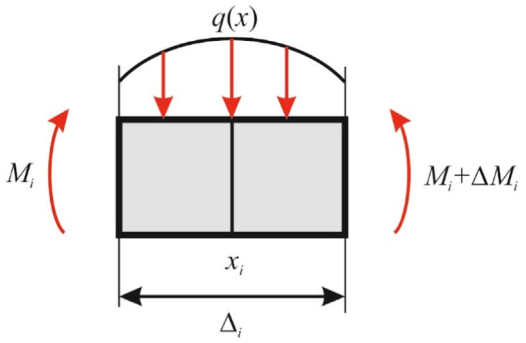

Fig. 9. Schematic view of the i-th inclusion.

normal displacement; $q = \frac{Q(lx)l^3}{k_0}$, $k_0 = E_0 I$; E_0 is Young's modulus of the beam material; I is the moment of inertia of the beam transverse cross section.

Let us isolate a small area around the i-th inclusion (Fig. 9).

In the case of a small concentration of the inclusions, the distances between them are essentially larger than their lengths. Therefore, $\Delta_i \ll 1$, and since $\Delta M_i \sim (\Delta_i)^2$, we take

$$\Delta M_i = 0, \tag{54}$$

$$M_i = k_i \left(\frac{d^2 w}{dx^2}\right)_{x=x_i}, \tag{55}$$

where: $k_1 = E_1 I$, E_1 is Young's modulus of the inclusion material.

Integration of the equation for equilibrium for elastic inclusion (Fig. 9) implies the following relations

$$(w)_{x_i-\Delta_i/2} - (w)_{x_i+\Delta_i/2} \sim (\Delta_i/2)^2; \left(\frac{dw}{dx}\right)_{x_i-\Delta_i/2} - \left(\frac{dw}{dx}\right)_{x_i+\Delta_i/2} \sim \Delta_i/2. \tag{56}$$

Relations (53)–(56) yield the following compatibility conditions assuming that $\Delta_i \to 0$:

$$\begin{cases} (M)^- = (M)^+; \left(\frac{dM}{dx}\right)^- = \left(\frac{dM}{dx}\right)^+; \\ (w)^- = (w)^+; \left(\frac{dw}{dx}\right)^+ - \left(\frac{dw}{dx}\right)^- = \left(\frac{k(x)}{k_0}\frac{d^2 w}{dx^2}\right)_{x=x_i}. \end{cases} \tag{57}$$

Bending moment M and deflection w are approximated by the following series

$$\begin{cases} M = M_0(x) + \varepsilon^2 M_1(x, \xi) + \cdots; \\ w = w_0(x) + \varepsilon^2 w_1(x, \xi) + \ldots, \end{cases} \tag{58}$$

where functions M_s, $w_s (s=1,2,\ldots)$ are periodic regarding ξ with a period n.

Using relations (53), (57), (58) yields the homogenized equilibrium equations of the FGM beam as well as the equation for the first corrector, which have the following forms

$$\frac{d^2}{dx^2}\left(\left(k_0 + \frac{k(x)}{n}\right)\frac{d^2 w_0}{dx^2}\right) = q; \frac{d^2 w_1}{dx^2} = \frac{1}{2}\left(q - k_0 \frac{d^4 w_0}{dx^4}\right)(\xi - n)\xi. \tag{59}$$

In the case of the FG steps between inclusions, we apply a function $f(x)$ (see Chapter 6), the fast variable $\xi = \eta/\varepsilon$, and, finally, the equilibrium equation, which overlaps with (59) when $k(x) = \varphi(x)$ is obtained.

11. Homogenized model of the FGM beam bending which adapts to the external load action

One of the challenging directions of the FG materials theory aims at constructing smart materials, which may change/adapt their characteristics in response to the action of external loads. As an example of a smart structure we consider a beam with inclusions which may change their sizes depending on action of the external load $q(x)$ (see Fig. 10a). The beam consists of the homogeneous material and n regularly distributed and stiff to bending inclusions having varying lengths. In what follows, we substitute action of the inclusions by their equivalent counterpart reactive moments, as it is schematically shown in Fig. 10b.

b) equivalent beam with the reactive moments M_i.

We assume that the magnitude of the reactive moments are proportional to the inclusion length and depends linearly on the rotation angle of the transverse beam cross section, in which the inclusion is located. We have

$$M_i = \left(k(x)\frac{dw}{dx}\right)_{x=x_i}. \tag{60}$$

Dimensionless equation governing beam bending (Fig. 10b) between two successive inclusions follows

$$\frac{d^4 w}{dx^4} = q. \tag{61}$$

On the other hand, compatibility equations on the i-th cross section can be written in the following form

$$(w)^- = (w)^+; \left(\frac{dw}{dx}\right)^- = \left(\frac{dw}{dx}\right)^+; \tag{62}$$

$$\left(\frac{d^2 w}{dx^2}\right)^+ - \left(\frac{d^2 w}{dx^2}\right)^- = k(x)\frac{dw}{dx}; \tag{63}$$

$$\left(\frac{d^3 w}{dx^3}\right)^+ - \left(\frac{d^3 w}{dx^3}\right)^+ = \frac{d}{dx}\left(k(x)\frac{dw}{dx}\right), \tag{64}$$

where: $k = \frac{lk_1(x)}{k_0}$, $k_1(x)$ is the coefficient of torsion rigidity of the inclusions.

Let us suppose $k(x) \sim \varepsilon$.

The deflection w is represented by the following series

$$w = w_0(x) + \varepsilon^4 w_1(x, \xi) + \varepsilon^5 w_2(x, \xi) + \cdots, \tag{65}$$

where: $w_s (s=1,2,\ldots)$ is periodic with respect to ξ function with the period n.

Introducing relations (4), (65) into Eq. (61) and compatibility conditions (62)–(64), and employing the splitting with respect to

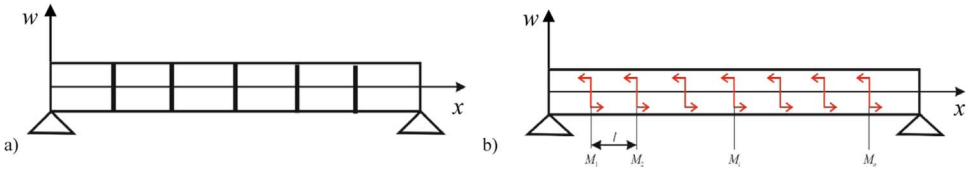

Fig. 10. Two beam models: a) beam with regularly distributed elastic inclusions of varying lengths;.

powers of ϵ, the following homogenized model taking into account the amplitude gradient is yielded

$$\frac{d^4w_0}{dx^4} + \frac{d}{dx}\left(k(x)\frac{dw_0}{dx}\right) = q. \tag{66}$$

12. Inverse problem

As an example, we find the optimal distribution of the inclusions providing the largest bending stiffness of the beam with constant total volume of inclusions, for a given load distribution q (x). As a target function $k(x)$ is taken. Observe that $k(x) \geq 0$, whereas $k(x)=0$ correspond to the beam parts without inclusions. In what follows, we introduce the auxiliary control function y such that $y^2 = k(x)$. We use the following isoperimetric condition

$$I_1 = \int_0^n y^2 dx = \widetilde{C}. \tag{67}$$

where $\widetilde{C}$ denotes a constant.

Therefore, the problem of an optimal design is reduced to find

$$I = \int_0^n w_0 q dx \to min_y; \tag{68}$$

$$\frac{d^4w_0}{dx^4} + \frac{d}{dx}\left(y^2\frac{dw_0}{dx}\right) = q. \tag{69}$$

For simplicity, we consider the boundary conditions of a simple support

$$w_0(0) = w_0(n) = 0; \left(\frac{d^2w_0}{dx^2}\right)_{x=0,n} = 0. \tag{70}$$

Applying variation of the Lagrange functional of the problem (67)–(70), and introducing the conjugate variable, we get the optimality condition

$$y\left(\left(\frac{dw_0}{dx}\right)^2 + \lambda\right) = 0. \tag{71}$$

13. An example of amplitude optimization

We consider the problem (67)–(71) for uniformly distributed external load $q = const$, $q \leq 0$. In this case we take into account the additional conditions of the central symmetry.

If we include the optimality conditions with respect to the second multiplier only, then the symmetry of the problem yields (71) on the interval $(0,\frac{n}{2})$, $\frac{dw_0}{dx} = \sqrt{-\lambda}$, and on the interval $(\frac{n}{2},n)$, $\frac{dw_0}{dx} = -\sqrt{-\lambda}$. Therefore, bending form of the optimal beam must have a node in the beam center $(x = \frac{n}{2})$. In order to avoid this, we introduce an additional, isolated central part (x_1, x_2), where the optimality condition will be satisfied with respect to the first multiplier $y=0$. The symmetry condition implies

$$x_2 = 1 - x_1. \tag{72}$$

In points x_1, x_2, the bending and deformation continuity hold (these conditions are derived by Weierstrass-Erdman relations [31])

$$\lim_{x\to x_{1,2}-0} w_0 = \lim_{x\to x_{1,2}+0} w_0; \lim_{x\to x_{1,2}-0} \frac{dw_0}{dx} = \lim_{x\to x_{1,2}+0} \frac{dw_0}{dx}. \tag{73}$$

Integrating the second multiplier of the optimality conditions (71) and taking into account the boundary conditions (70), the deflections on both $(0,x_1)$, (x_2, n) intervals are found

$$w_{01} = \lambda_1 x, \quad x \in (0,x_1); w_{02} = \lambda_1(n - x), \quad x \in (x_2, n), \tag{74}$$

where $\lambda_1 = \sqrt{-\lambda}$.

From Eq. (69) for $y=0$ one obtains

$$w_{03} = q\frac{x^4}{24} + C_1x^3 + C_2x^2 + C_3x + C_4, \tag{75}$$

where $C_i (i=1-4)$ are constants.

Substituting (74), (75) into (73) and taking into account symmetry condition (72), C_i and λ_1 can be expressed by the variable x_1 in the following form

$$C_1 = -\frac{qn}{12}; C_2 = 0; C_3 = \frac{qn^3}{24}; C_4 = \frac{qx_1^3}{2}\left(\frac{x_1}{4} - \frac{n}{3}\right); \tag{76}$$

$$\lambda_1 = \frac{q}{24}(n^3 - 6nx_1^2 + 4x_1^3). \tag{77}$$

Introducing (74) into (69), we may define the control function $y(x)$on the interval $(0,x_1)$, (x_2, n). The boundary conditions for the target function are chosen in the following way

$$y(0) = y(n) = 0, \tag{78}$$

which means that there are no inclusions on the boundaries. As a result, the target function is a piecewise function of the following form

$$y^2 = \begin{cases} \frac{24x}{n^3 - 6nx_1^2 + 4x_1^3}, & x\epsilon(0, x_1); \\ 0, & x\epsilon(x_1, n - x_1); \\ \frac{24(n-x)}{n^3 - 6nx_1^2 + 4x_1^3}, & x\epsilon(n - x_1, n). \end{cases} \tag{79}$$

It should be emphasized that the target function does not depend on the magnitude of the external load, which is typical for linear problems.

Implementing expression (79) into the isoperimetric condition (67), one obtains equation for x_1

$$\frac{\widetilde{C}}{24}(n^3 - 6nx_1^2 + 4x_1^3) - x_1^2 = 0. \tag{80}$$

The graph of the size of the central zone of the beam free of inclusions to total value of the inclusions $\widetilde{C}$less than $n = 10$ is shown in Fig. 11. The values of x_1 are yielded by Eq. (80) in a unique way, as the positive root is less than $n/2$. The shape of the target function $y^2$for the beam subjected to the uniformly distributed load for $n=10$,$\widetilde{C}=5$, is reported in Fig. 12.

Therefore, the deflection of the optimally supported beam is governed by a continuous function

$$\overline{w} = \begin{cases} \frac{1}{24}(n^3 - 6nx_1^2 + 4x_1^3)x, & x\epsilon(0,x_1); \\ \overline{w}_{03}, & x\epsilon(x_1, n - x_1); \\ \frac{1}{24}(n^3 - 6nx_1^2 + 4x_1^3)(n - x), & x\epsilon(n - x_1, n), \end{cases} \tag{81}$$

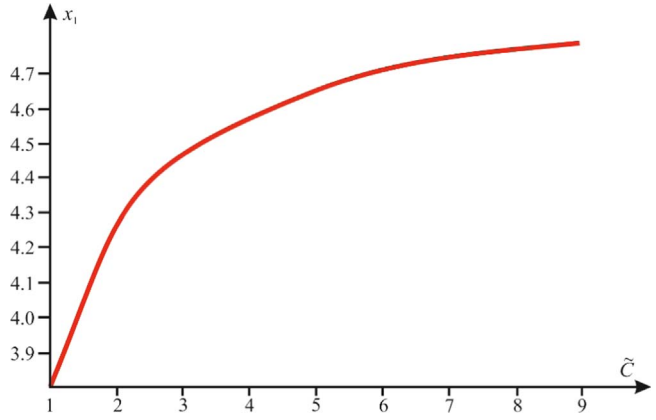

Fig. 11. Coordinate x_1 (the beginning of the central beam zone without inclusions) vs. $\widetilde{C}$ for $n=10$; $q = const$..

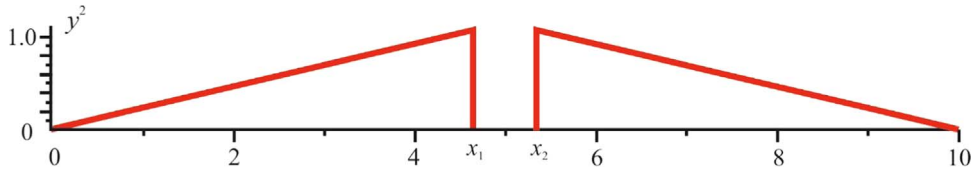

Fig. 12. The target function $y^2(x)$ regarding bending of the optimal simply supported FGM beam subjected to a uniform load (n=10,$\widetilde{C}$=5); (x_1, x_2) is the zone without inclusions, x_2=n–x_1.

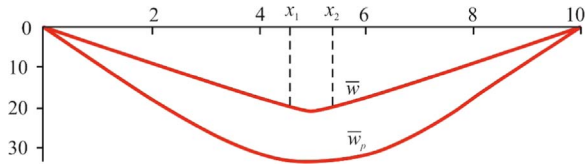

Fig. 13. Beam deflection under the external uniform load action (n=10,$\widetilde{C}$=5): $\overline{w}_p$ for the regular structure; $\overline{w}$ for the optimal FG structure; (0, x_1), (x_1, 10) are the intervals corresponding to the straight beam axis position; (x_1, x_2) is the bended beam part.

$$\text{where: } \overline{w} = \frac{w_0}{q}; \overline{w}_{03} = \frac{x^4}{24} - \frac{qn}{12}x^3 + \frac{n^3}{24}x + \frac{x_1^3}{2}\left(\frac{x_1}{4} - \frac{n}{3}\right).$$

The beam deflection (81) for n=10,$\widetilde{C}$=5 is shown in Fig. 13, which includes the deflection of the regular beam (reinforced by the same inclusions) yielded by the following ODE:

$$\frac{d^4 w_p}{dx^4} + k\frac{d^2 w_p}{dx^2} = q, \tag{82}$$

where $k = \widetilde{C}/n$.

Integrating Eq. (82) and taking into account the boundary conditions (70) for n=10,C=5, one obtains

$$\overline{w}_p = \frac{4sin\left(\frac{x}{\sqrt{2}}\right) - 4sin\left(\frac{x}{\sqrt{2}} - 5\sqrt{2}\right)}{sin(5\sqrt{2})} + x^2 - 10x - 4, \tag{83}$$

where $\overline{w}_p = \frac{w_p}{q}$.

Comparison of the maximum deflections of the optimal FGM beam $\overline{w}(\frac{n}{2})$ and the regular composite beam $\overline{w}_p(\frac{n}{2})$ shows that the proposed optimization sufficiently increases the beam stiffness.

14. Concluding remarks

Introduction of the function f(x) allowed solving problems of computations and optimal design of FGS with a FG inclusion sizes and FG steps between inclusions using the unique approach. Both considered problems occurred to be identical from the mathematical point of view, whereas the difference between them is in the sense of coefficients in the constitutive equations and control functions.

While optimizing the FGS with FG inclusion sizes and FG steps between inclusions, it is recommended to look for the control function on a set of piecewise continuous functions. The optimization process is realized with the help of two mechanisms. First of all, we define the boundary area where inclusions do not occur. Secondly, we choose inclusion sizes to fit the external load distribution. The reported optimization mechanisms, being obvious from physical point of view, have found a mathematical foundation in our work. It is expected that the proposed method will be useful during computations and optimal design of more complex heterogeneous structures governed by differential equations of a higher order.

In addition, the carried out analysis of the simply supported FGM beam subjected to uniformly distributed pressure (Fig. 13) yields the following observations. The beam deflection takes place only in the central part of the beam, on the interval (x_1, $n - x_1$). The length of the remaining non-reinforced beam part $2x_1$ decreases while the total stiffness of the inclusions C is raised (see Fig. 11). Therefore, an increase in the total stiffness of inclusions implies an increase in the beam stiffness. However, it should be mentioned that problems for other boundary conditions or for other loads require additional investigations.

Acknowledgments

This work has been supported by the Polish National Science Centre, MAESTRO 2, No. 2012/04/A/ST8/00738.

References

[1] S. Suresh, Graded materials for resistance to contact deformation and damage, Science 292 (2001) 2447–2451.
[2] D.L. Holl, Stress transmission on earths, Proc. Highw. Res. Board 20 (1940) 709–772.
[3] K. Hruban, The basic problem of a non-linear and non-homogeneous half-space, Non-Homogeneity in Elasticity and Plasticity, W. Prager, Pergamon Press, New York, 1958, pp. 53–61.
[4] B. Ilschner, N. Cherradi (Eds.), Proceedings of the 3rd International Symposium on Structural and Functional Gradient Materials, Lausanne, Switzerland, 1994.
[5] S. Suresh, A. Mortensen, Fundamentals of Functionally Graded Materials, Institute of Materials, London, 1998.
[6] T. Hirai, Functionally gradient materials (Processing of Ceramics), in: R.J. Brook (Ed.), Materials Science and Technology, 17B VCH Verlagsgesellschaft, Weinheim, Germany, 1996, pp. 292–341.
[7] Functionally Graded Materials, Proceedings of the 5th International Symposium on FGM, in: W.A. Kaysser (Ed.), Dresden, Germany, Trans. Tech. Publ., Switzerland, 1998 (1999).
[8] L. Wang, S. Rokhlin, Universal scaling functions for continuous stiffness nanoindentation with sharp indenters, Int. J. Solids Struct. 42 (13) (2005) 3807–3832.
[9] A. Bensoussan, J.-L. Lions, G. Papanicolaou, Asymptotic Analysis for Periodic Structures, North-Holland, Amsterdam, 1978.
[10] E. Sanchez-Palencia, Non-Homogeneous Media and Vibration Theory, Springer-Verlag, Berlin, 1980.
[11] N.S. Bakhvalov, G.P. Panasenko, Averaging Processes in Periodic Media Mathematical Problems in Mechanics of Composite Materials, Kluwer Dordrecht, 1989.
[12] G.P. Panasenko, Multi-Scale Modeling for Structures and Composites, Springer-Verlag, Berlin, 2005.
[13] I. Babushka, The computation aspects of the homogenization problem, Lect. Notes Math. 704 (1979) 309–316.
[14] I.V. Andrianov, J. Awrejcewicz, L.I. Manevitch, Asymptotical Mechanics of Thin-Walled Structures: A Handbook, Springer-Verlag, Berlin, Heidelberg, 2004.
[15] A.G. Kolpakov, Stressed Composite Structures: Homogenized Models for Thin-Walled Nonhomogeneous Structures with Initial Stresses, Springer-Verlag, Berlin, New York, 2004.
[16] L.I. Manevitch, I.V. Andrianov, V.G. Oshmyan, Mechanics of Periodically Heterogeneous Structures, Springer-Verlag, Berlin, Heidelberg, New York, 2002.
[17] A.B. Movchan, N.V. Movchan, C.G. Poulton, Asymptotic Models of Fields in Dilute and Densely Packed Composites, Imperial College Press, London, 2002.
[18] A. Anthoine, Second-order homogenisation of functionally graded materials, Int. J. Solids Struct. 47 (2010) 1477–1489.
[19] T. Reiter, G. Dvorak, V. Tvergaard, Micromechanical models for graded composite materials, J. Mech. Phys. Solids 45 (8) (1997) 1281–1302.
[20] I.V. Andrianov, J. Awrejcewicz, A.A. Diskovsky, Homogenization of the irregular cell-types constructions, in: J. Awrejcewicz, D. Sendkowski, Mrozowski (Eds.), Proceedings 8th Conference on Dynamical Systems - Theory and Applications, Lodz, pp. 871–876, 2005.
[21] I.V. Andrianov, J. Awrejcewicz, A.A. Diskovsky, Homogenization of quasiperiodic structures, Trans. ASME J. Vibr. Acoust. 128 (4) (2006) 532–534.
[22] I.V. Andrianov, J. Awrejcewicz, A.A. Diskovsky, Asymptotic investigation of corrugated elements with quasi-periodic structures, in: J. Awrejcewicz, M. Kaźmierczak, P. Olejnik, J. Mrozowski (Eds.), Proceedings 10th Conference on Dynamical Systems – Theory and Applications, Lodz, 523-532, 2009.
[23] I.V. Andrianov, J. Awrejcewicz, A.A. Diskovsky, Design of the non-homogeneous quasi-regular structures, in: V.I. Bolshakov, D. Weichert (Eds.), Advanced Problems in Mechanics of Heterogeneous Media and Thin-walled Structures, ENEM, Dnipropetrovs'k, 2010, pp. 7–18.
[24] I.V. Andrianov, J. Awrejcewicz, A.A. Diskovsky, Homogenization of the function-

ally-graded materials, in: J. Awrejcewicz, M. Kaźmierczak P. Olejnik, J. Mrozowski (Eds.), Proceedings 11th Conference on Dynamical Systems – Theory and Applications, Lodz, 55-62, 2011.
[25] I.V. Andrianov, J. Awrejcewicz, A.A. Diskovsky, Sensitivity analysis in design of constructions made of functionally-graded materials, Proc. Inst. Mech. Eng. Part C: J. Mech. Eng. Sc. 227 (1) (2013) 19–28.
[26] I.V. Andrianov, V.V. Danishevs'kyy, H. Topol, D. Weichert, Homogenization of a 1D nonlinear dynamical problem for periodic composites, ZAMM 91 (6) (2011) 523–534.
[27] M. Goland, E. Reissner, The stresses in cemented joints, J. Appl. Mech. 11 (1944) A17–A27.
[28] G. Geymonat, F. Krasucki, S. Lenci, Mathematical analysis of a bonded joint with a soft thin adhesive, Math. Mech. Solids (1999) 201–225.
[29] R.W. Hamming, Numerical Methods for Scientists and Engineers, McGraw Hill, New York, 1962.
[30] N.V. Banichuk, Introduction to Optimization of Structures, Springer-Verlag, New York, 1990.
[31] E.F. Masur, Singular problems of optimal design, in: E.J. Haug, J. Cea (Eds.), Optimization of Distributed Parameter Structures, Sijthoff-Noordhoff, Iowa, Alphen aan den Rijn, 1980, pp. 200–218.